World Academy of Science, Engineering and Technology
International Journal of Mechanical and Mechatronics Engineering
Vol:11, No:1, 2017

A Xenon Mass Gauging through Heat Transfer Modeling for Electric Propulsion Thrusters

A. Soria-Salinas, M.-P. Zorzano, J. Martín-Torres, J. Sánchez-García-Casarrubios, J.-L. Pérez-Díaz, A. Vakkada-Ramachandran

***Abstract*—**The current state-of-the-art methods of mass gauging of Electric Propulsion (EP) propellants in microgravity conditions rely on external measurements that are taken at the surface of the tank. The tanks are operated under a constant thermal duty cycle to store the propellant within a pre-defined temperature and pressure range. We demonstrate using computational fluid dynamics (CFD) simulations that the heat-transfer within the pressurized propellant generates temperature and density anisotropies. This challenges the standard mass gauging methods that rely on the use of time changing skin-temperatures and pressures. We observe that the domes of the tanks are prone to be overheated, and that a long time after the heaters of the thermal cycle are switched off, the system reaches a quasi-equilibrium state with a more uniform density. We propose a new gauging method, which we call the Improved PVT method, based on universal physics and thermodynamics principles, existing TRL-9 technology and telemetry data. This method only uses as inputs the temperature and pressure readings of sensors externally attached to the tank. These sensors can operate during the nominal thermal duty cycle. The improved PVT method shows little sensitivity to the pressure sensor drifts which are critical towards the end-of-life of the missions, as well as little sensitivity to systematic temperature errors. The retrieval method has been validated experimentally with CO_2 in gas and fluid state in a chamber that operates up to 82 bar within a nominal thermal cycle of 38 °C to 42 °C. The mass gauging error is shown to be lower than 1% the mass at the beginning of life, assuming an initial tank load at 100 bar. In particular, for a pressure of about 70 bar, just below the critical pressure of CO_2, the error of the mass gauging in gas phase goes down to 0.1% and for 77 bar, just above the critical point, the error of the mass gauging of the liquid phase is 0.6% of initial tank load. This gauging method improves by a factor of 8 the accuracy of the standard PVT retrievals using look-up tables with tabulated data from the National Institute of Standards and Technology.

***Keywords*—**Electric propulsion, mass gauging, propellant, PVT, xenon.

I. Introduction

THE effective use of propellant on spacecraft is vital to ensuring the successful completion of the spacecraft mission goals and to create viable mission extension options. Using propellant effectively is essential to have an accurate knowledge of the remaining propellant mass. Propellant gauging is critical to the end date of a mission and therefore to the profit that a satellite operator will make, as well as for the planning of long-time operation missions in the context of telecommunication or space exploration. Additionally, an accurate knowledge of the density flow is a key variable for two thruster performance parameters: specific impulse and efficiency. Thus, any method that can accurately determine the density has the potential to be used not only for End of Life (EOL) prediction but also for efficient propulsion and station-keeping management.

In the new era of space missions, the EP is becoming an increasingly popular option. EP is safer than the traditional chemical propulsion, and furthermore, EP engines are more efficient in the sense that they require much less propellant to produce the required spacecraft impulse. The propellant is ejected up to 20 times faster than that of classical thrusters, and therefore, the same propelling force is obtained with 20 times less propellant. The electric thrusters work with very small flows, so that they push the spacecraft very gently compared to other more traditional options such as chemical systems. On the other hand, the force that it produces can be applied continuously for very long periods – months or even years and it is thus a highly reliable option for interplanetary trips. They can as well be used to regulate the thrust provided to the spacecraft with extremely high precision, and thus allow controlling the its orientation and position along the orbit with much better precision [1]. The EP is currently being proposed, in modern telecom or scientific satellites, as the only propulsion system on-board, and to be used both for orbit transfers and station keeping stages. The use of EP on a modern telecommunications satellite easily provides a saving of more than 20% in the initial launch mass. Today's most important applications of EP are the sector of geostationary telecommunications satellites, such as ESA's Artemis, where the technology is used to move the satellite from its initial transfer orbit to its final orbit around the Earth and to maintain that orbit throughout the satellite's operational lifetime of 10 to 15 years. The second important use of EP is for interplanetary probes, such as the ESA's SMART-1 probe to the Moon or the Bepi-Colombo missions to Mercury, where EP provides the primary source of thrust for transporting the satellite to its final destination [1].

The most common pressurized propellant is xenon. Its low ionization energy and high atomic mass make xenon suitable for this propulsion system, with favorable energy to thrust ratio. Its relatively low critical pressure of 58.4 bar is also an advantage, given the fact that above this pressure it is possible

A. Soria-Salinas, M.-P. Zorzano, J. Martín-Torres and A. Vakkada Ramachandran are with the Atmospheric Sciences Group, Department of Computer Sciences, Electrical and Space Engineering, Luleå University of Technology, Kiruna 98128 (BOX 848) Sweden (phone: +46 (0)980 67536, email: alvaro.tomas.soria.salinas@ ltu.se).

J. Sánchez-García-Casarrubios and J.-L. Pérez-Díaz are with the Department of Signal and Telecommunication Theory, Universidad Autónoma de Madrid, 28049 Madrid, Spain.

This study has been partially funded by the Swedish National Space Board.

to store the propellant as a supercritical fluid, instead of gas, with an extremely high density. This allows storing a larger mass of propellant within the same given volume.

The lifetime of the new EP missions may be as long as 10 to 15 years. As a result, the size of xenon propellant tanks on-board has substantially augmented to increase its storage capabilities from the initial 200-350 kg to 800-1500 kg. Since the propellant is continuously consumed during the mission it is critical to ration its use and to know the remaining mass in the tank with the best possible accuracy. The precise knowledge of the propellant remaining mass is thus a truly competitive factor, since the spacecraft lifetime is one of the most important variables that determines the success and profitability of a mission. For instance, a failure in the estimate of the remaining mass at the EOL may lead to a catastrophic failure in the final orbital maneuvers or to originate the impossibility of correcting or even aborting the operations previously performed.

At the Beginning of Life (BOL), right after fueling on the ground segment, xenon is stored in a tank, at pressures above the critical point and in supercritical stage. This propellant is then used during the mission in a continuous way for different maneuvers of the spacecraft. As the propellant mass is consumed slowly, the remaining mass in the tank needs to be gauged by some robust measuring technique that is not sensitive to sensor degradation through its long operational lifetime.

The mandatory requirements are thus to have a robust mass gauging method that: a) can retrieve the mass of propellant in the tank in the absence of gravity; b) properly performs throughout the large density and pressure variations that take place from BOL to EOL with a technology that has been qualified for space; and c) it is easily scalable for different tank sizes. Xenon is stored in pressurized tanks in a unique state (i.e. either gas or liquid, with no liquid-gas interface). Other potential gases for EP that can be stored with this same philosophy are krypton (Kr), argon (Ar), helium (He) and nitrogen (N_2).

In this document, we present an improved hybrid gauging method for EP systems, and we discuss the main error sources, illustrate the densities anisotropies induced by the transfer of heat, and present an experimental validation within a chamber that has been specifically built for this purpose.

II. Requirements and Pitfalls of Gauging Methods

The remaining mass within spacecraft's propellant tanks is usually retrieved through several gauging methods in parallel [2], [3]:

a) Propellant Bookkeeping (i.e., estimating propellant usage during each maneuver and subtracting the used amount from initial propellant mass estimates),
b) Pressure-Volume-Temperature (PVT) measurements (i.e., the use of the pressure and temperature telemetry data to calculate the mass by using the relationship of pressure-volume-density and the tank volume),
c) Thermal Gauging (i.e., approximating mass through analysis of propellant system temperature telemetry during given heat inputs). For a comparative review of these methods, see [2], [3]. Some of them are more suitable for the initial stages of a mission, such as Bookkeeping and PVT methods, whereas Thermal Gauging behaves better at EOL stages, but all of them lead to large errors especially at the end of mission [4]-[7].

In this work, we summarize a new proposed method for xenon (or other gases) mass gauging. The gauging method and its technology shall be compatible with the following requirements:

1) Designed for gaseous/supercritical applications assuming high purity xenon and other potential EP propellants such as He, Ar, Kr, or N_2.
2) Be operative for ground storage and stand-by at launch pad, for three to five months long cruise phase to the geostationary orbit (GEO) and for the orbiting phase in GEO orbit without gravity pull.
3) Withstand the space environment in terms of: temperature (T), pressure (P), radiation, vibrations, spinning configuration, absence of gravity (for GEO orbit), etc.
4) Cope with the space qualification processes: thermal vacuum, electromagnetic compatibility, radiation exposure, depressurization, vibration, and shock testing.
5) Require little or none maintenance.
6) Avoid movable parts if possible.
7) Provide information that can be easily interpreted in real time and included in telemetry data packages.
8) Be constraint in terms of mass and volume (and ideally data and power).
9) Consider redundancy.
10) Rely on robust components with heritance in space flight and expected long lifetimes of at least five years on ground, 15 years in space with the possibility to extend up to 18 years.
11) Show little sensitivity to critical alignments or positioning of parts.
12) Require no (or have limited amount of) consumables.
13) Pose no risk to other elements in the platform and ground-segment operators during fueling.
14) Be scalable to higher density/pressure/volume ranges foreseen for future applications.
15) Be compatible with the thermal duty cycle which is applied to the tank where the propellant is stored within a lower and upper temperature limit. In particular, we consider as reference a maximum xenon storage temperature allowed at any time is 50 ºC and minimum xenon temperature allowed at any time is 20 ºC with a thermal duty cycle within 38 °C and 42 °C.
16) Most importantly any new method should ideally be based on in-flight tested physical principle and technologies (and thus have a high TRL).

We take as starting point the classical PVT gauging method because it complies with most of the points above, and it is based on simple measurements and on basic physical principles which are universal. Next, we summarize some of the main issues of this method:

1) In most of the cases the ideal gas law is used to describe the fluid contained in pressured tanks during the whole range of operation, including supercritical, or phase change stages. Some previous attempts for improving this aspect have been found in the early stages of the THEMIS spacecraft constellation [4].
2) Other cases rely on National Institute of Standards and Technology (NIST) tabulated data of P, T, and density (ρ) and take the T and the skin of the tank and the P of the sensors as input to retrieve a density value that is supposed to be homogeneous throughout the tank [8].
3) The pressure transducer errors and EOL systematic drifts as consequence of its progressive degradation along the mission cause density retrieval errors. Simultaneous comparisons with other gauging methods are currently used to mitigate the uncertainties induced by this issue.
4) As the propellant tanks content depletes and the pressure load decreases, the sensitivity of the method to small changes in density (i.e., mass) through pressure changes is reduced, increasing the errors in the retrieval. It becomes critical at the EOL stage, where the best accuracy is required.
5) The temperature gradients within the tanks as consequence of heterogeneous heat load application, external uncontrolled thermal loads from the environment and lack of convection are neglected. The temperature sensors are located only at certain points of the external skin of the tanks; however, a uniform fluid temperature for the whole tank content is usually used by averaging external temperatures that are only representative of certain regions. As we shall demonstrate in Section III, the shape of the tank also originates undesirable overheating at the tank skin, and finally, all these factors lead to density anisotropies.

III. Heat Transfer Problem: Thermal and Density Anisotropies

As stated in the previous section, the different temperatures within the tank lead to different densities. To illustrate this and understand what it is the best regime where our proposed method can be applied, we have developed CFD simulations of the heat transfer in a representative tank. The density changes with T and P, and this, as we shall show, will affect the heat transfer by inducing mass flows within the tank. The primary purpose of this simulation is to obtain qualitative information about the order of magnitude of inner temperature anisotropies and density differences within the tank. Furthermore, we want to investigate the role of the tank geometry to detect hot-spots and provide crude estimates of the transient times for stabilization. In order to investigate the influence of the density variation alone and to avoid further external sources of anisotropies for the examples shown, here no solid tank has been included, and no thermal fixed boundary conditions (i.e., belts, supporting points) are imposed. The P, T, and ρ properties of xenon for the investigating ranges shall be changed according to the NIST data. This allows calculating the behavior of the xenon at liquid state and its progressive conversion to gas state whenever the tank is being emptied, allowing for a more realistic heat transfer modeling of the complete process. The thermal problem should include the solution of the Navier-Stokes problem. We choose COMSOL® software to investigate this case. This program is very robust for heat transfer studies, and allows to tabulate the properties of the gas/fluid (xenon) and to impose a thermal loop control. It also allows for future improvements, including different materials, convection caused by gravity, or conduction to the orbiter and radiation-mediated heat transfer. But, most importantly, it models as well the pressure, temperature and density distributions all over the model and derives the velocity field. For this simulation, we have used the Heat Transfer Module whose main purpose is to correctly model the heat transfer in solids and fluids. Given the extensive database of materials that the program has, it is clearly useful for the future modeling of materials of the layers and the xenon itself. By adding the Mechanical Module, the mechanical properties of the solid layers can be included and mechanical deformations induced by temperature and pressure in the tank structure can also be investigated.

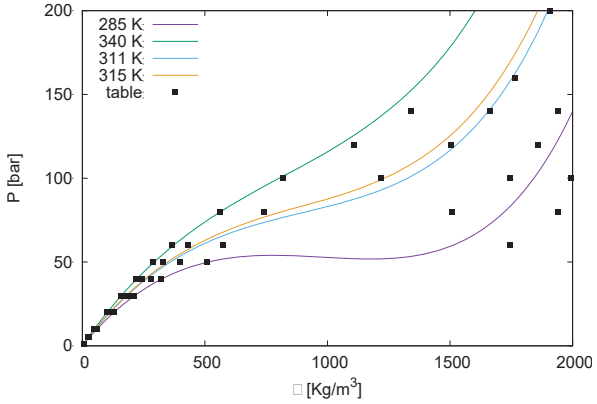

Fig. 1 Pressure variation with density for different temperatures and tabulated data for the COMSOL® CFD simulation of xenon storage within the tank

The fluid within the tank is xenon whose specific heat at constant pressure $C_p(T)$ and thermal conductivity $k(T)$ are tabulated for the simulation and vary with temperature according to the properties described in NIST. A thermal control point has been located in the center of one of the hemispheric caps (or "domes") because, as we shall show, this is the region that heats the most. To simulate a standard thermal duty cycle, a heating loop is programmed in COMSOL® that is on when the temperature is lower than 42°C, and switches on when it cools below 38°C. The heating loop is implemented assuming that either 10 or 30 W are applied uniformly to the tank walls. The time evolution of the density field is obtained by solving the Navier-Stokes equations. The corresponding P-T-ρ relationships are taken from a tabulated file for linear interpolation which is again obtained from the NIST database for xenon. The data used for tabulated information are shown in Fig. 1 (data points) and

compared with a smooth fit for the nominal case of the theoretical full formulation. As expected, for low pressures, the conditions are similar to the ideal gas case. Figs. 2 and 3 show the time evolution of the cross-section map of the temperature for two different pressure regimes. These temperature gradients lead to local density differences and to inner propellant mass flows. An example of this flow is shown in Fig. 4. Fig. 5 shows the time evolution of the temperature as it would be sensed by some hypothetical sensors placed at the dome of the tank, or the center of the xenon volume, compared with the average temperature of the xenon propellant.

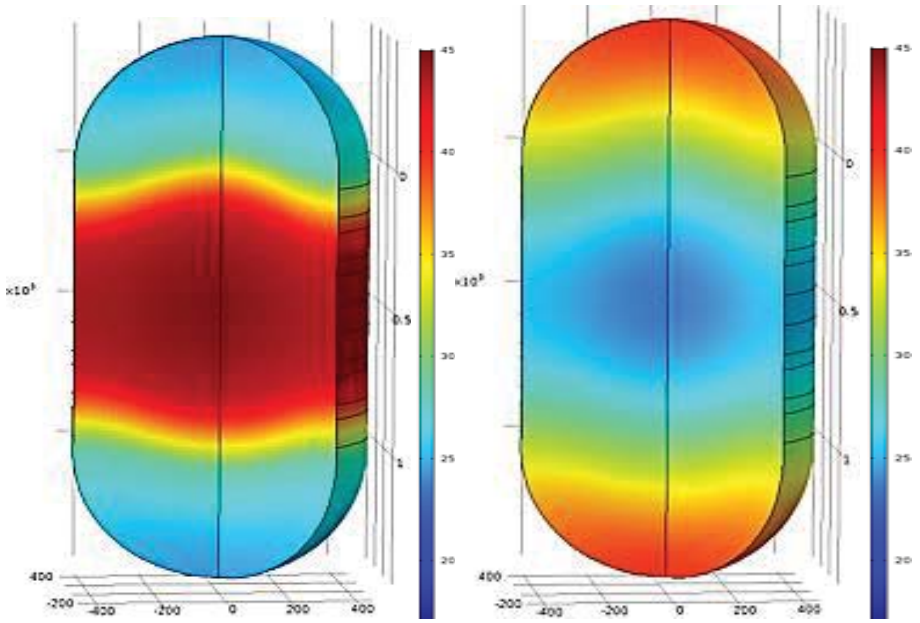

(a) (b)

Fig. 2 Vertical cross-section of a simulated xenon elongated tank at pressure of 2 bar (EOL scenario), where a thermal duty cycle is applied. Temperature (and density) anisotropies distribution in ^{o}C. Initial condition at 20 °C and 10 W uniformly applied to the external boundary of the integrating volume: (a) after 1h; (b) after 5h

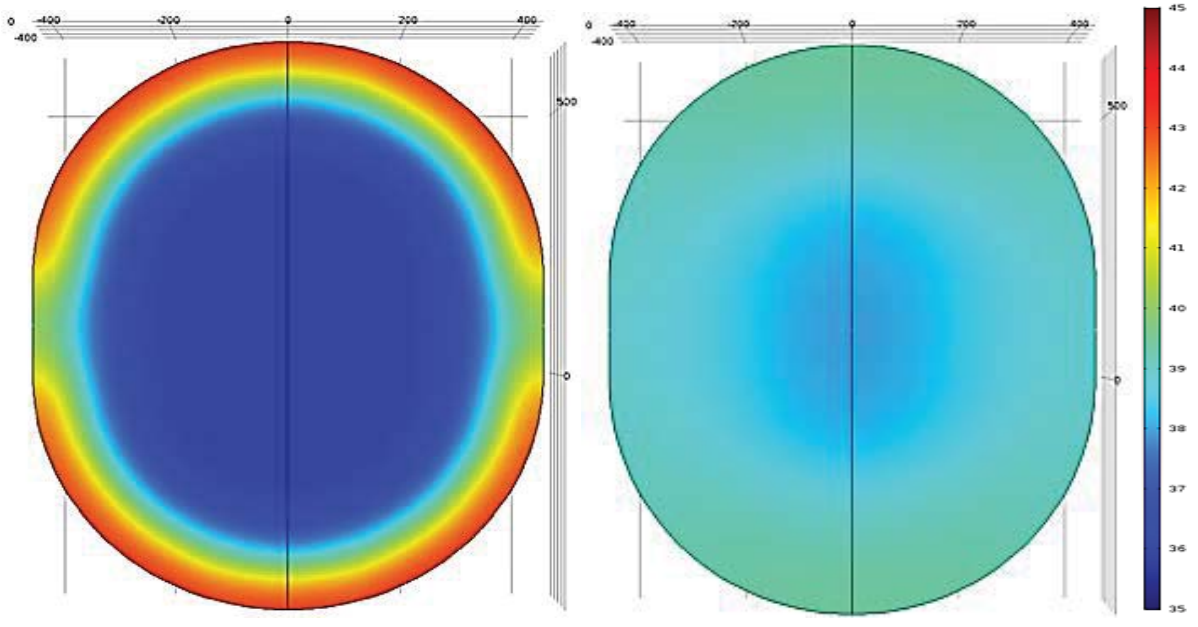

(a) (b)

Fig. 3 Vertical cross-section of a simulated xenon tank at pressure of 100 bar (BOL scenario), where a thermal duty cycle is applied. Temperature (and density) anisotropies distribution in ^{o}C. Initial condition at 36 °C and 30 W uniformly applied to the external boundary of the integrating volume: (a) temperature profile after 1 day; (b) temperature profile after 10 days. After 18 days, the thermal profile is uniform (not shown)

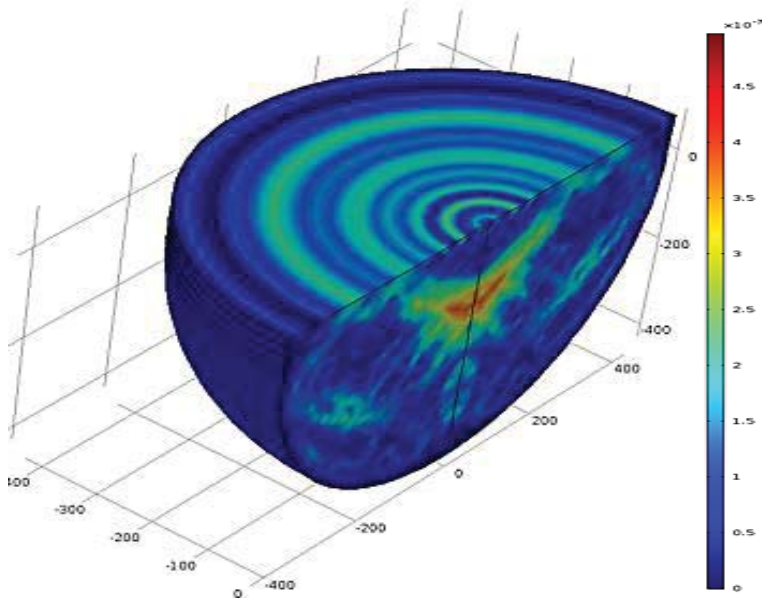

Fig. 4 Velocity field of the propellant within the xenon tank of Fig. 3 in $m \cdot s^{-1}$ after 10 days

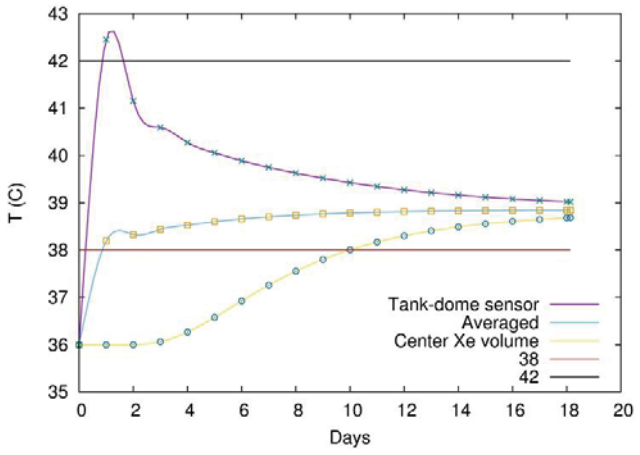

Fig. 5 Evolution of temperature probe points within the xenon tank of Figs. 3 and 4

During the thermal ramp shown in Fig. 5, there is an increase in P and a large density increment within the tank. Then, as the heating power is turned off, and the system is left to cool down, the thermal gradients disappear, the pressure decreases and the system behaves in a quasi-stationary way reaching an almost uniform density state.

According to the preliminary CFD simulations the thermal gradients produced by the external heating system can induce big density differences at these high P-ρ ranges and in big volumes. In particular, because of the geometry of the tank, the hemispheric caps will be at higher temperature and lower density. This effect increases for larger lengths of the tank (Fig. 2 versus Fig. 3), even in the case of ideal gas. This may hinder the usage of thermal gauging methods for the BOL, since they assume density uniformity throughout the heating phase. For instance, after one day of heating in the case at P of 58 bar, there is a gradient of density of 1%.

It is thus important to feed the thermal control loop system with reference temperatures from the hot-spot regions, and to have pressure sensors that measure simultaneously. Otherwise the temperature may go above the desired limit within the domes (it happened for some simulations where the control point for the thermal loop was set on the sides), and the hot-spots of the tank may risk the safe operation of this system. In order to retrieve the density accurately even in the case of anisotropies, we suggest to monitor the temperature from the domes to the central areas of the tank, and ideally also inside the tank.

When the initial conditions are set to 36 °C with an initial pressure of 100 bar, it takes about 10 days to heat all the Xe above the temperature threshold limit, and about 18 days to reduce the temperature differences within the tank to below 0.3 °C.

The goal of this work is to propose a method that based on the existing sensing technology (namely, P and T monitoring on the outer shell of the tank) can provide information about the density status inside the tank and then, by multiplying it by the tank volume, about the remaining mass. We will focus our research on the cooling phase where the system is expected to be in pseudo-equilibrium state with more uniform densities. The physical principle of the proposed method shall be described in the following section.

IV. Improved Gauging Method from Redlich-Kwong Equation

We suggest using the Redlich-Kwong equation to describe the xenon behavior within the tank, either in fluid or gaseous state:

A. PVT-RK Method

$$P = \frac{R\rho T}{(M-b\rho)} - \frac{1}{T^{1/2}} \frac{a\rho^2}{M(M+b\rho)} \quad (1)$$

where P represents the pressure of the fluid contained, T its

temperature, ρ the fluid density that we need to retrieve, R the universal gas constant, M the molecular mass, and a and b two constants that are identified depending on which gas is being analyzed. Equation (1) applies to all the operational range. In physics and thermodynamics, the Redlich–Kwong equation of state is an empirical, algebraic equation that relates temperature, pressure, and volume of gases. It is generally more accurate than the Van der Waals equation and the ideal gas equation at temperatures above the critical temperature. It was formulated by Otto Redlich and Joseph Neng Shun Kwong in 1949 [9]. It showed that a two-parameter, cubic equation of state could well reflect in reality in many situations, standing alongside the much more complicated Beattie–Bridgeman model and Benedict–Webb–Rubin equation that were used at the time. The Redlich–Kwong equation has undergone many revisions and modifications, in order to either improve its accuracy in terms of predicting gas-phase properties of more compounds, as well as in better simulating conditions at lower temperatures, including gas–liquid equilibria. In this case, however, we use it for single phase propellants, i.e. either gas bellow the critical point or liquid. Some values for the most important gases are summarized in Table I.

Despite the fact that (1) was used in the very early EP development for designing the storage of spacecraft tanks [9], its application fell into disuse, with some punctual application in space missions in the recent years [4], which concede to this fluid description certain heritage.

TABLE I
SUMMARY OF RESULTS FROM SUPERCRITICAL CHAMBER EXPERIMENTS

Critical values	H	He	Ar	Kr	Xe
Normal Boiling point (NBP) [K]	20.384	4.125	87.29	119.8	165.0
Density at NBP [kg · m^{-3}]	67.0	124.8	1392	2412	3080
Critical pressure [bar]	33.24	5.20	150.7	209.4	289.74

Instead, ideal gas or bi-cubic interpolation from Xe-NIST database is usually used [10]. This realistic description is more suitable for a gas stored at high pressures, especially at supercritical stage. The true advantage of (1) is that it allows for a continuous representation of the state of the xenon during the whole lifetime of a spacecraft. It also allows calculating analytically the role of P and T inaccuracies and degradations in the final mass retrieval. Finally, and thanks to (1), an analytical description for the fluid density at each pressure within the tank can be estimated along the whole life of the mission. In particular, for the storage of xenon we take as nominal thermal range 38 °C to 42 °C for the thermal duty cycle and a pressure range of 0 to 100 bar. As it can be observed in Fig. 6, the behavior of pressurized xenon when the density grows is totally different from the ideal gas approach. It can be seen as well the decrease of the slope of the curves when the fluid approaches and pass the critical point (represented with the vertical red line). The slope of this intermediate stage is also different depending on the temperature of the fluid, being higher as the fluid temperature increases.

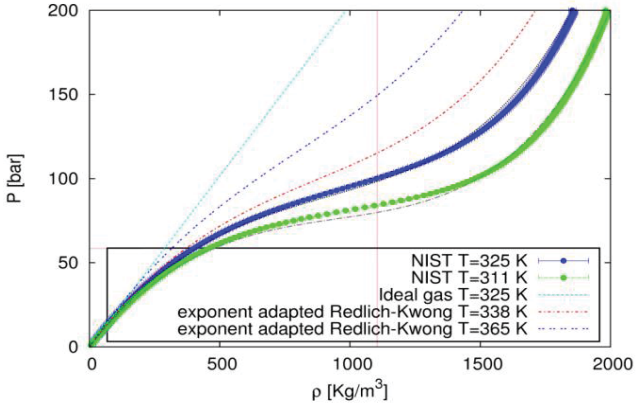

Fig. 6 Comparison of the pressure-temperature-density curve for the ideal gas law case and the NIST data base for xenon, for different temperatures. Comparison of an adapted version of the Redlich-Kwong equation of state against NIST data up to the range of supercritical conditions and T sensitivity

In the case of propellant stored within a fixed volume, when T is changed under isochoric conditions with an external heating or cooling phase this induces a change in P. Both P and T are measured simultaneously by independent sensors that are outside the xenon propellant bulk media. Xenon state is now fully described through the analytical expression (1), and we can derive this expression with respect to the fluid temperature, obtaining a new equation for the isochoric behavior:

B. Delta-Method

$$\frac{dP}{dT} = \frac{R\rho}{(M-b\rho)} + \frac{1}{2}\frac{1}{T^{3/2}}\frac{a\rho^2}{M(M+b\rho)} \quad (2)$$

Equation (2) represents the expected infinitesimal pressure change that shall be experienced in a stored system at a given density when an infinitesimal temperature change is applied. The tanks are continuously exposed to a temperature heating cycle followed by a cooling cycle. This is not only observed at the temperature pattern of the skin of the tank but also at the pressure measured by the P sensors of the tank. The ratio of change of P with respect to the change of T is thus also a measurable quantity that should be unique for each density of the contained xenon.

Equation (2) is not sensitive to pressure sensor error drifts since it depends on the difference between two consecutive measured values and the subtraction between them cancels out any systematic error. It is furthermore less sensitive to the specific operational temperature than (1) (since it only depends on the second additive term through a $T^{-3/2}$ dependency) and we foresee that it will be more robust and less dependent on instrument measuring errors. As it has been shown in the CFD simulation, we expect that when a pseudo-stationary equilibrium is reached (2) shall describe the system as a whole. In particular, during the cooling phase, when no active heating is applied, and the system is left to equilibrate itself, the change in pressure versus thermal variation should be unique for all the system parts, both inside and at the shell

of the xenon tank.

Equations (1) and (2) are non-linear, i.e. on the contrary to the ideal gas law, where ρ, P or T can be obtained immediately from a simple equation, here (1) or (2) must be solved numerically to retrieve ρ, P, or T from the knowledge of the other two variables. We have implemented a numerical solver to find the solution of (1) and (2) for each set of measured values. In the PVT-RK method (1), an error in the P or T measurement leads to a direct error in the density retrieval. In the Delta method (2), an error in the P or T measurements has a different influence depending on its nature. Systematic errors in P and T cancel out in the Delta-method on the left side of the equation: $(P_2 - P_1)/(T_2 - T_1)$. However, the systematic error in T has an influence on the right-hand side of the equation where the density is, and this leads to an error in density. Pressure errors drifts are the most critical ones for the PVT-RK method or other standard PVT methods [2], as seen Fig. 7. However, these are not relevant for the Delta-method.

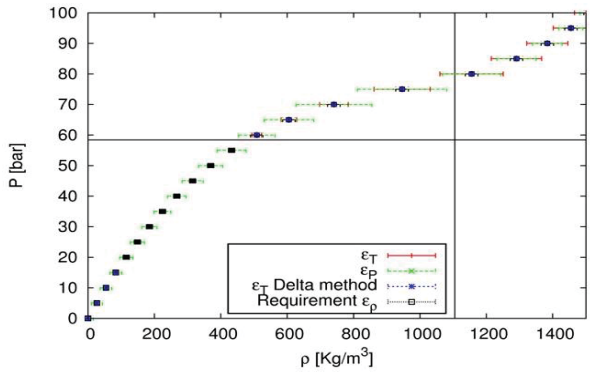

Fig. 7 Analysis of expected errors caused by a systematic error of 2 K in the temperature measurements (ε_T) and of 3 bar in pressure measurement (ε_P), during a typical life-time density variation, from 0 to 100 bar. The Delta-method is far more robust with respect to systematic errors

V. Validation under Laboratory Conditions: Supercritical Chamber

An experimental chamber has been built for testing the Improved PVT gauging method early exposed, which uses the combined analysis of the PVT-RK and Delta-method. The main goal of this chamber is to demonstrate the validity of this gauging method and to quantify the magnitude of internal and external thermal gradients. To simplify the tests and costs of the experiment and without loss of generality, the tests are performed with pressurized CO_2. This is a gas that is very frequently manipulated in supercritical conditions and which has a similar behavior to xenon. The critical pressure point of CO_2 is 73.8 bar. Some views of this chamber, called 'Supercritical Chamber', are shown in Figs. 8-10. The Supercritical chamber consists of a 1.55 liters stainless steel vessel suitable for 100 bar pressure (up to 250 bar), with three Pt100 temperature sensors inside, and two external pressure sensors, external heaters (see the orange stripes in Fig. 9), and thermal insulation. This chamber can hold gas/fluid in supercritical stage at varying temperature regimes. The volume deformation is monitored with strain gauge sensors. The system includes a manually operated valve for alleviation of CO_2 and connector to a CO_2 bottle of pressurized has. A data acquisition card (DAC) for pressure, deformation in volume, and temperature is included to register the data in real time.

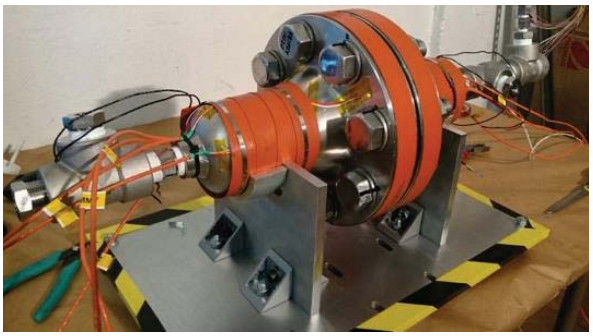

Fig. 8 View of the 'Supercritical Chamber'. The orange tapes that surround the structure correspond to the heating strips through which the thermal cycle is applied. The external Pt100 temperature and strain gauge sensors attached to the chamber skin are visible, with the PID control at the clamp

Fig. 9 Thermal insulation material cover

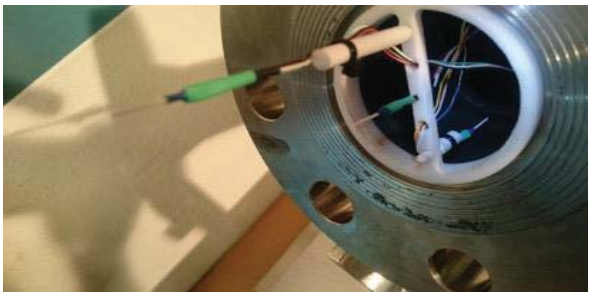

Fig. 10 Internal view of the opened 'Supercritical Chamber'. Three temperature sensors are attached to a white Teflon structure which a negligible thermal conductivity. These sensors are used to monitor the temperatures inside the gas

The chamber is composed of two stainless steel halves joint by a clamp in order to introduce the sensing elements within the tank at the central section. The full system is mounted on a bascule for calibration of the CO_2 injected mass. Previous simulation analysis through CFD studies confirmed the

presence of overheating regions as consequence of the tank shape at the dome regions. Consequently, the internal sensing elements were placed as far as possible from the perturbations originated at the domes (Fig. 10). Both sides of the chamber have high precision pressure transmitters 'PTX 600 Series', with one of them connected through tubing to the exterior for CO_2 injection and closed by a valve. The thermal insulation material is critical to avoid excessive losses to the ambient, to emulate the spacecraft configuration of the tank, and to use more efficiently the heating system by reducing the radiative and convective thermal losses to the ambient (Fig. 10). The whole assembly counts with seven Pt100 temperature sensors distributed both inside the tank, attached to the Teflon structure, and at the external skin, a PID control for heating cycles, and strain gauge sensors for volume changes measurements. The bascule has a precision of 1 g over a full range of 60 kg, pressure and temperature sensors have accuracies of 0.03% at full scale and 0.06 K (1/10DIN) respectively, and the strain gauge sensors can detect variations of 0.15% over the full-length scale.

A. Preliminary Description and Sensor Performance

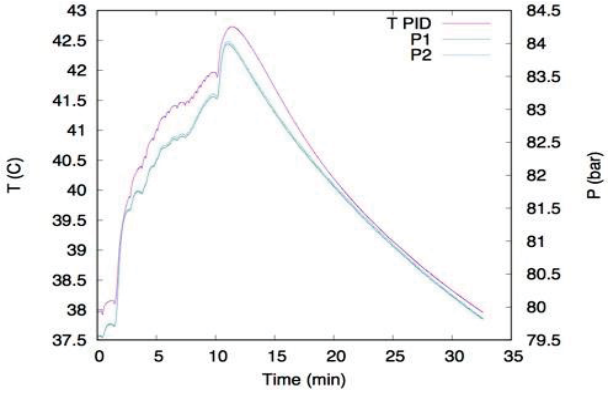

Fig. 11 Time evolution of the two pressure transducers and the PID temperature control sensor during a heating cycle in the range of 82 bar and vertical configuration

Following the experimental procedure, different pressures have been chosen to characterize the method at all regimes found in a hypothetical lifetime of a spacecraft. An example of one of the thermal cycles applied to the chamber can be seen in Fig. 11.

The pressure transducers show a highly similar behavior during a nominal heating and cooling ramp. This heating is controlled by the PID temperature sensor. The heating is not applied continuously, but step by step in order to avoid too high local overheating and heaters degradation. In Fig. 12, the same cycle is represented as a function of time through all temperature sensors measurements.

The heterogeneous behavior of the fluid temperature distribution within a tank during thermal cycles can be clearly seen in Fig. 12. This takes place even under Earth convective heat transfer, which favors the homogenization in temperatures all over the tank. Both temperature sensors located at the domes show a high sensitivity to the power injection steps during the heating ramp since they are closer to the heaters than the rest of the sensors and because of the geometric effect mentioned before. In addition, since the configuration in this case is vertical, a clear stratification is observed along the internal and PID temperature sensors. This vertical stratification is caused by convection that appears on Earth because of gravity, but it does not appear in the space configuration. Thus, for the final analysis, the tests will be performed on horizontal configuration. Notice that despite the temperature limits established at the thermal control loop (at 42.7 °C), the tank is overheated up to 60 °C, and thus, hot spots are unavoidable in this kind of configurations. Here, a heating by steps is clearly demonstrated to be needed in order to avoid high overheating in the domes. These overheating peaks observed are not seen by the control heating loop, which could lead to dangerous situations for a spacecraft tank.

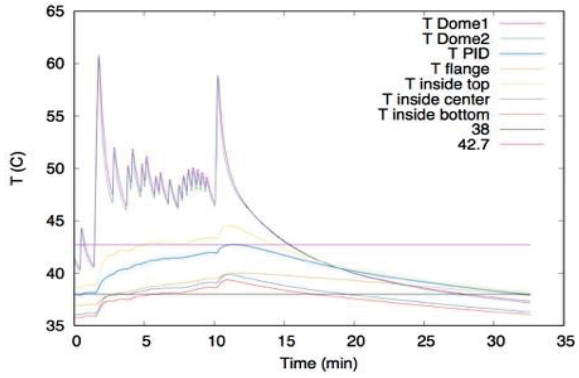

Fig. 12 Time evolution of several temperature sensors during a test with vertical configuration of the inner sensors and PID temperature sensor in the range of 82 bar and vertical configuration

The deformation of the propellant tank volume in space is usually calculated from laboratory calibrations of the volume increment with pressure. An example of this deformation can be observed in Fig. 13. The gas temperature differences are large, in particular in the vertical dimension. This is seen in the temperatures that are monitored by the sensors attached to Teflon structure in both horizontal and vertical configurations (see Fig. 15). The vertical gradients within 15 cm can be as large as 40 °C during the heating ramp. This is caused by the effect of gravity and convective cells. When the system reaches a pseudo-stationary state during the cooling phase, this is reduced to about 4 °C for the vertical stratification. The horizontal temperature differences are well below 0.08 °C.

In addition to this expected linear change with pressure, the short strain gauges of the volume are very sensitive to rapid temperature changes, as it can be observed in Fig. 14. This is not usually taken into account in the space configuration. None of these deformations are significant for our experimental setup with a thick dense stainless steel chamber, but it may be significant for the space configuration since propellant tanks are characterized by thin walls that can be deformed with local overheating. As a result, they may induce errors in all the mass gauging procedures that rely on density calculation.

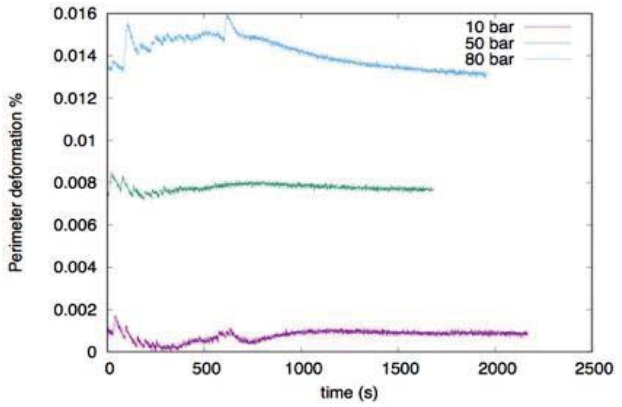

Fig. 13 Comparison of chamber deformation during heating cycles tests at three different initial pressures in % of initial diameter

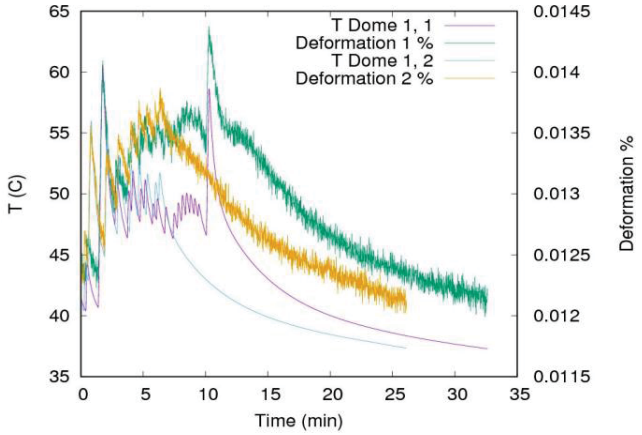

Fig. 14 Temperature retrieval at the dome 1 of the chamber and tank deformation during the initial heating ramp in % of initial diameter

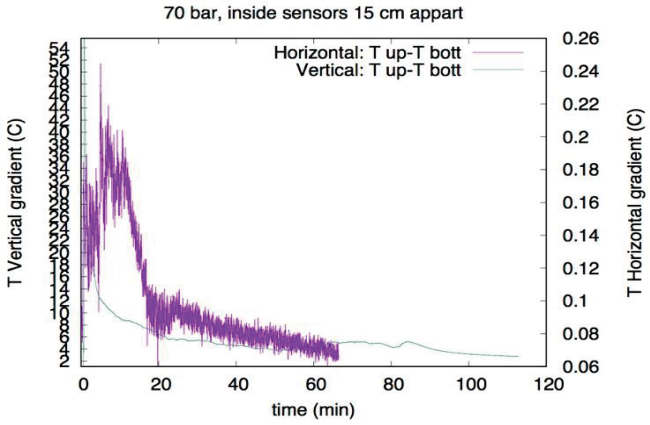

Fig. 15 Inner gas temperature differences as monitored by the sensors attached to Teflon structure in both horizontal and vertical configurations

The pressure sensing systematic differences between the two pressure sensors have also been detected in the Supercritical Chamber, see Fig. 16. They are presumably caused by their different operating temperatures and their calibrated temperature correction functions. Fig. 16 shows a variability of the pressure drifts estimated as the subtraction of the two pressure sensor measurements along the tests. An upper limit of ± 0.05 bar could be set. However, when the tested pressure corresponds to the critical point one, 73.8 bar in case of CO_2, the differences between sensors strongly increase, with differences up to 0.15 bar shown in Fig. 17.

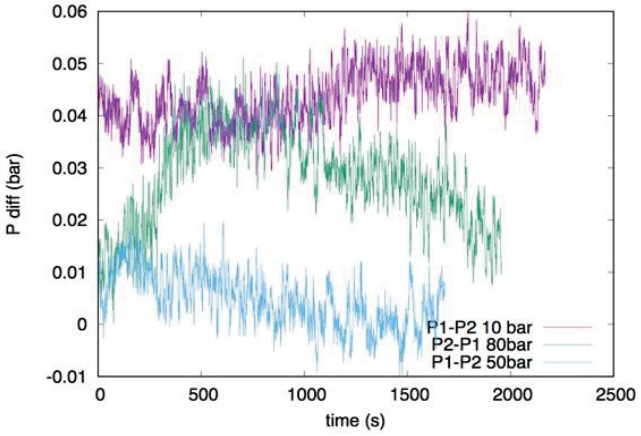

Fig. 16 Pressure transducers difference tendencies between the two pressure transducers at the Supercritical Chamber for different initial pressures

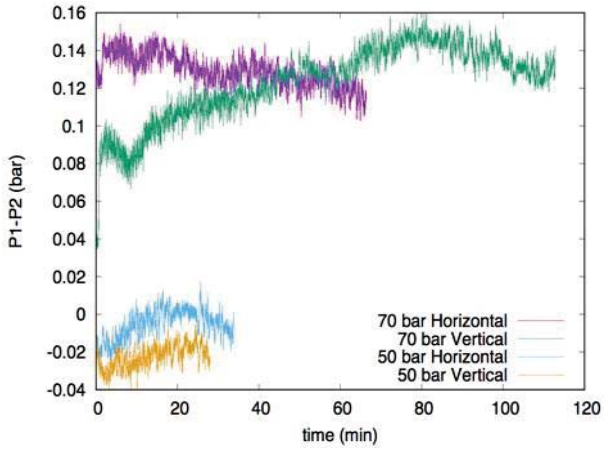

Fig. 17 Pressure transducers difference at critical pressure comparison with a lower pressure case for both horizontal and vertical configurations

Fig. 18 represents the noise level observed for pressure transducers and PID temperature control sensor, with an upper limit of ± 0.005 bar and ± 0.005 K at the stabilized stage, respectively. This noise variability is calculated by subtracting two consecutive values of measured *P* or *T*.

B. Results

Once the operational limits of the chamber have been analyzed, some experiments are run with CO_2. The goal of these tests is to measure the mass of the CO_2 inside the chamber using (1) and (2) and to compare the retrieved value with the weight obtained through the 1 g resolution bascule. Some examples of the typical *P-T* data curves are shown in Fig. 19. In these tests, we show experiments that are run under horizontal or vertical configuration conditions. These graphs

show the evolution of pressure versus temperature for each of the temperature sensors. The last minutes of the data acquired by the PID sensor are marked in green, during the phase of cooling when the quasi-stationary state is reached. During this phase, at the end of the cooling ramp, the slope of the *P* versus *T* variables is the same for the sensors inside, and the sensors on the outer shell of the tank. This means that here the Delta *P*/Delta *T* measured at the tank can be used as a proxy for what it is actually the behavior of the full system and can therefore be used, with (2), to estimate the mass.

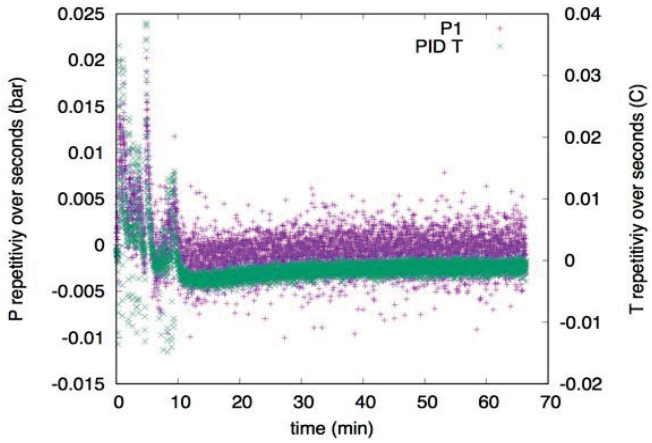

Fig. 18 Pressure and temperature noise level

The overheating developed in the vertical configuration is clearly seen as indicated by the *T*-up temperature sensor attached to the internal cross section assembly (Fig. 19 (a)). This overheating does not take place on the horizontal plane. The presence of convection generates this stratification that would take place on-orbit in case of having a constant acceleration at a certain direction or as a consequence of a thruster ignition. After the initial heating, the system is left to cool down freely and it can be observed the convergence to the initial values before the heating, when the temperature of the assembly arrives to the initial point. The Delta-method would be used during the cooling stage, represented at Fig. 20 as f(x). The horizontal test is assumed to represent on-orbit scenario where gravity does not act, and convection is not present.

C. Analysis of the Experimental Data with the Improved PVT-RK Method and Delta-Method Comparison with NIST PVT Method

Fig. 20 shows the expected theoretical curve, according to (1) and (2), for the range of densities and masses considered here for CO_2. The data points are the corresponding values obtained from the experiments. Three experiments are run for each study case (most of the results are overwritten in the plot, because the tests are very reproducible). The inner sensors and the external PID temperature sensor are placed on a horizontal configuration to avoid the influence of gravity-induced convection.

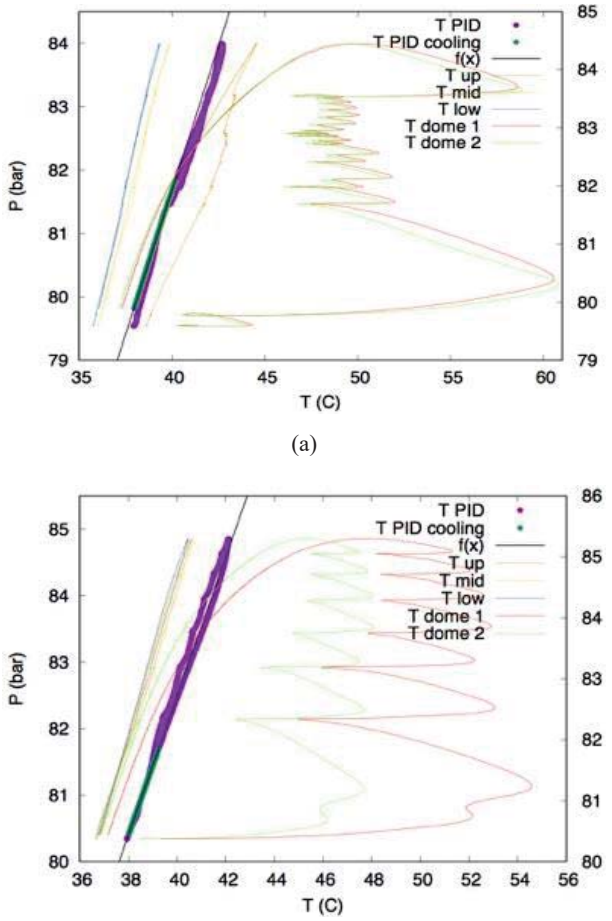

Fig. 19 Delta-method measured variables for a 0.520 g CO_2 mass stored up to 80 bar: (a) in vertical configuration; (b) in horizontal configuration

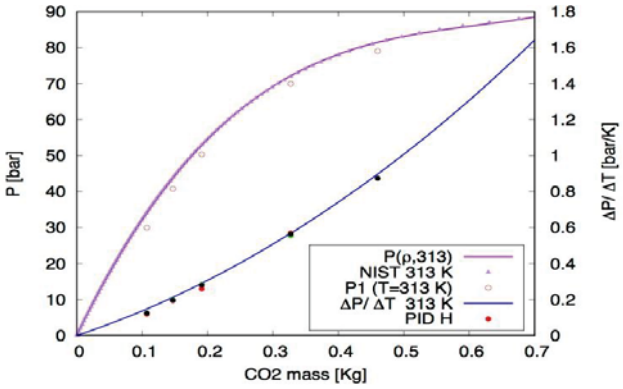

Fig. 20 PVT-RK (Redlich-Kwong equation) and Delta-method analytical expression for the range of CO_2 mass established. Comparison of theoretical estimations with experimental results summarized in Table II

At each test, the pressure measured at the stabilized cooling stage, when temperature in the PID control point is 40 °C, is annotated. On the other hand, the Delta *P*/Delta *T* method during the end of the cooling phase is applied. An example of the typical experimental products obtained at different

horizontal configurations is summarized in Table II. These results are then compared for all the three experiments per mass range with the theoretical curves for P versus ρ (and mass), and Delta P/Delta T versus ρ (and mass) for a volume of V=1.55 L.

TABLE II
SUMMARY OF RESULTS FROM SUPERCRITICAL CHAMBER EXPERIMENTS

CO_2 mass [kg]	P at 40°C [bar]	PID slope [bar · K^{-1}] last 20 min
0.184	51.913280	0.332371
0.300	69.979483	0.573537
0.520	81.595617	1.044070

The measured values are then used to solve numerically (1) and (2) and to retrieve the density ρ, and from here assuming a uniform distribution the mass within the volume V. Figs. 21 and 22 show a comparative analysis between the two retrieval methods exposed and the data directly interpolated from NIST database once we measure the PID control temperature and the pressure at a 77 bar case, i.e. CO_2 supercritical state and 70 bar (gas). These data have been first averaged over 60 seconds or 120 seconds and analyzed in real time to prove the validity to gauge the mass within a short time spam of about 4 minutes. Regarding the NIST database, a linear interpolation has been used to derive the density values. Then, the PVT-RK method has been used by fitting the Redlich-Kwong equation of state for the averaged P and T (every two minutes) readings and solved for density, and the same has been done for the Delta-method (2). As it can be seen in Fig. 22, the error in the CO_2 mass retrieval for both NIST and PVT-RK methods is about 40 g, which later usually leads to smaller errors. On the other hand, Delta-method shows an error in this retrieval of about 5 g. Considering the 460 g of injected CO_2 into the chamber at supercritical state, in Delta-method, we are retrieving the mass with a 1.1% of the initial mass accuracy error. If we extrapolate this scenario to propellant storage conditions within a spacecraft tank, and by assuming that the initial mass of the system would have been injected at 100 bar (as it is the case for xenon propellant), then this tank, when it is full of CO_2 (i.e., at launch conditions), would have had 955 g of CO_2 (for our 1.55 L chamber). Thus, with the Delta-method, we can give the contained CO_2 mass with a 0.5% accuracy of the initial mass, either for CO_2 or xenon, at launch conditions considering that at this stage the tank is pressurized at 100 bar (which is the case). As a result, this gauging method improves by a factor of 8 the accuracy of the original NIST-based PVT retrieval with a TLR-9 technology and without being sensitive to systematic P-drift errors. Since the weight balance accuracy (and rounding) error is 1 g, we cannot obtain an error better than 1 g in the retrieval.

Alternatively, we can analyze the mass by taking all the data of the cooling phase, i.e. by analyzing the data of the last 25 minutes up to the point when the temperature reaches 35°C. Fig. 22 represents a situation just below the supercritical state, at 70 bar. Using all the data the error is further reduced, and this can be improved if the results of multiple experiments (i.e., multiple cooling ramps) are used. A summary of this is summarized in Table III, for 70 bar, and IV, for various pressures including supercritical conditions at 77 bar.

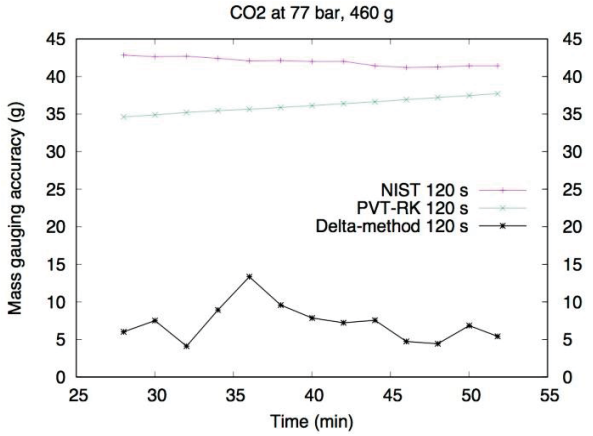

Fig. 21 Comparative error analysis between NIST interpolated data, PVT-RK method and Delta-method in mass retrieval for 460 g of CO_2 at 77 bar

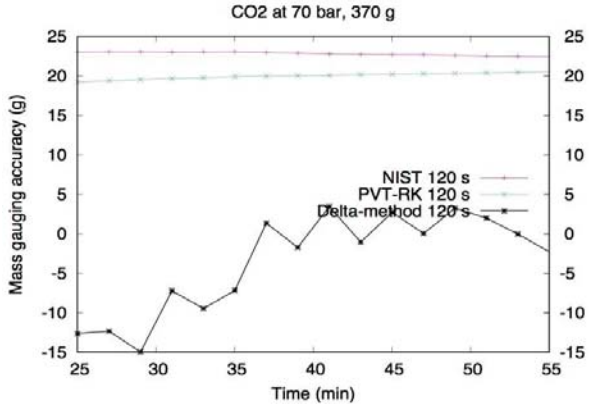

Fig. 22 Comparative error analysis between NIST interpolated data, PVT-RK method and Delta-method in mass retrieval for 370 g of CO_2 at 70 bar

TABLE III
70 BAR, 35 °C. SUMMARY OF RESULTS FROM SUPERCRITICAL CHAMBER EXPERIMENT ERROR

Slope Nº	1	2	3	Average
Delta P/Delta T (20 min. cooling)	0.5707	0.5535	0.5635	0.5626
Retrieved mass [g]	329,68	321,97	326,48	326,04
Calibrated mass [g]	327	327	327	327
Error mass [g]	**-2,68**	**5,03**	**0,52**	**0,96**
Error mass [%]	**-0,82**	**1,54**	**0,16**	**0.29**

TABLE IV
SUMMARY OF RESULTS FOR GASEOUS AND SUPERCRITICAL STAGE

Mass (g)	P range (bar)	Mass Error av. (g)	Mass Error av. %	Mass Error av. % (995 g BOL)	Density Error (kg · m^{-3})
147	40	9,33	6,35	**0,98**	**6,0**
191	50	8,17	4,28	**0,86**	**5,3**
327	70	0,96	0,29	**0,10**	**0,62**
460	77	6,08	1,3	**0.64**	**3,9**

VI. Conclusions

We have proposed a new gauging method that is based on the use of the equations of the state of gases and fluids. One of the most popular propellants for future EP applications is xenon, but this method applies also to other such as helium, argon, and krypton, as well as other gases such as CO_2. The retrieval method has been presented and demonstrated experimentally. This method can be easily adapted to any EP tank, for other geometries, sizes and gases. It has to be said that convection effects were not removed in this chamber and further analysis would require a complete study in microgravity conditions. The role of impulses and transients should also be further investigated in a gravity-less platform. Finally, in the future, the chamber can be adapted to tests for other gases such as nitrogen, helium and xenon.

This method uses only the *T* and *P* readings of sensors that are placed on the outside of the tank and can operate during the nominal thermal duty cycle of the heating systems of the pressurized propellant tanks. This method relies thus on existing TRL-9 technology. The equations are universal, they can be applied to multiple gases and their use is scalable provided that a quasi-stationary state is reached. The Delta-method shows little sensitivity to the pressure sensor drifts that are critical towards the EOL of the missions and shows little sensitivity to systematic temperature errors too.

The heat transfer problem that is representative for the xenon propellant tank has been investigated with a CFD code. The relevance of the thermal anisotropies on the density has been explained qualitatively with computational simulations that integrate the Navier-Stokes equations and the hot-spots of the system have been identified.

It is here demonstrated that the temperature distribution within de fluid can be different, sometimes even significantly larger than the one sensed on the side of the tank by the PID thermal control temperature, as expected from previous simulations. Even after long term stabilization, the thermal gradients inside the gas can be as high as 3 or 4 K within 15 cm in the vertical dimension (because of Earth gravity and convection). Within the small chamber and within a distance of 15 cm, we observe a gradient of 0.06 K horizontally. The vessel deformation amplitude increases linearly with *P*, but also shows dilatation with T. When this is important for the tank volume change, it should be calibrated as a function of *T* and *P*.

Because the system is always out of equilibrium, the temperature sensed at the surface is not always representative of the inside temperatures (and densities). However, in the cooling phases the slopes Delta *P*/Delta *T* of all the elements converge. Both the PVT-RK and the Delta-method, with a nominal thermal-duty cycle, can be used to gauge the mass once a pseudo-equilibrium has been reached (i.e., on the cooling ramp). The Delta-method, with long cooling ramps and horizontal configuration, works better than the classical PVT gauging method at gas and supercritical state. The error in the mass retrieval is demonstrated to be lower than 1% of the initial mass within the tank, considering this initial loading at 100 bar. In this line, for a pressure just before the critical pressure of CO_2 of 70 bar, the error in the retrieval at this gas phase state is reduced to 0.1%, whereas just above the CO_2, critical `pressure, at 77 bar, the error in this superfluid case is 0.6%, both in comparison to the initial tank load. This gauging method improves by a factor of 8 the accuracy of the original NIST-based PVT retrieval with a TLR-9 technology and without being sensitive to systematic *P*-drift errors. Notice that the mass for lower pressure ranges is really negligible with regard to the weight of the full experimental chamber (45 kg) and thus for lower pressures it is understandable that the error is larger. Finally, this method gives the density with very good accuracy and thus it can be used to determine the flux and for efficient propulsion and station-keeping management.

Acknowledgment

The authors gratefully acknowledge the financial support given for this work by the Swedish National Space Board (NRFP-3 Call), COMSOL® advisors and OHB-Sweden for their interest on this topic.

References

[1] European Space Agency, "*Electric Propulsion; Technology Programs*." BR-187, July 2002.

[2] B. Yendler, "Review of Propellant Gauging Methods," *AIAA 2006-939; B9 SpaceOps Conference*, 2012.

[3] B. Hufenbanch et al., "Comparative Assessment of Gauging Systems and Decription of a Liquid Level Gauging Concept for a Spin Stabilised Spacecraft." ESA SP-398.561H, Aug. 1997.

[4] B. D. Owens, D. Cosgrove, M. Sholl, M. Bester, "On-Orbit Propellant Estimation, Management, and Conditioning for the THEMIS Spacecraft Constellation." *AIAA 2010-2329; SpaceOps Conference*, 2010.

[5] I. Oz, L. Pelenc, B. Yendler, "Thermal Propellant Gauging, SpaceBus 2000 (Turksat 1C) Implementation," *AIAA 2008-7697; SPACE Conference and Exposition.*

[6] M. E. Ahmed, O. Nemri, B. Yendler, S. Chernikov, "Implementation of Thermal Gauging Method for SpaceBus 3000A (ArabSat 2B)," *AIAA 2013; DOI: 10.2514/6.2012-1269441*.

[7] B. Yendler, W. S. Lawson, A. R. Cheuvront, G. McAllister, "Fuel Estimation for Stardust-NExT Mission," *AIAA-2010-8712*.

[8] National Institute of Standards and Technology-NIST WebBook- "Thermophysical Properties of Carbon dioxide," http://webbook.nist.gov/cgi/fluid.cgi?ID=C124389&Action=Page (accessed October 2016).

[9] R. Welle, "Propellant Storage Considerations for Electric Propulsion," *AIAA-91-2589*, 1991.

[10] S. Pessina, S. Kasten-Coors, "In-Flight Characterisation of Cryosat-2 Reaction Control System," *22nd International Symposium on Space Flight Dynamics*, 2011.